ORGANIC LETTERS

2011
Vol. 13, No. 19
5334–5337

Synthesis and Evaluation of a Fluorescent Ritterazine–Cephalostatin Hybrid

Kanduluru Ananda Kumar,[†] James J. La Clair,*[,‡] and Philip L. Fuchs*[,†]

Department of Chemistry, Purdue University, West Lafayette, Indiana 47907, United States, and Xenobe Research Institute, P.O. Box 3052, San Diego, California 92163-1052, United States

i@xenobe.org; pfuchs@purdue.edu

Received August 13, 2011

ABSTRACT

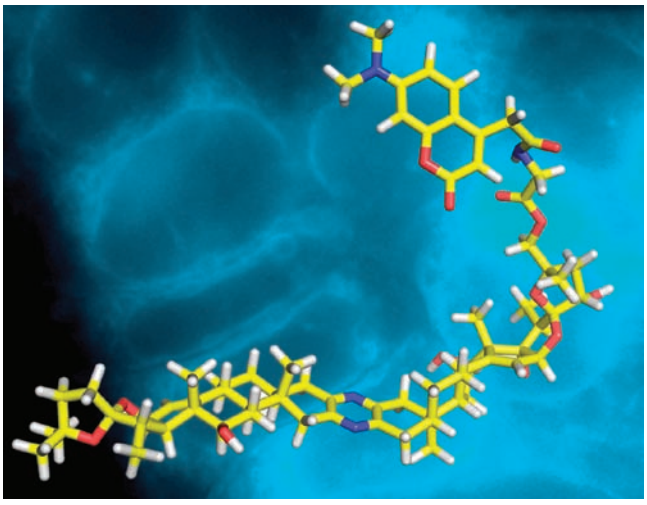

The cephalostatin and ritterazine natural products comprise a potent family of bis-steroidal pyrazines that display potent single-digit nanomolar inhibition of tumor cell growth. An active fluorescent ritterazine–cephalostatin hybrid probe was developed using detailed SAR data derived through total synthetic efforts. A combination of time course and confocal imaging studies indicate that this natural product family is rapidly taken up in tumor cells and localizes subcellularly within ER and surrounding the nuclear–ER interface.

Ritterazine B (**1**) is a member of a large family of natural products (over 45 cephalostatin and ritterazine congeners) that were isolated from marine organisms by the laboratories of Pettit[1a] and Fusetani.[1b] The unique structure of these bis-steroidal compounds (see Figure 1) along with their potent single-digit nanomolar inhibition of tumor cell growth is highlighted by an average GI_{50} value of 1.2 nM for cephalostatin 1 (**2**) in the NCI-60 cell line screen. This potent activity along with their unique cell selectivity and apoptotic response has drawn attention to their potential as clinical leads for cancer.[2]

Soon after their isolation, synthetic programs were launched, with the first total synthesis reported in 1995.[3] While these synthetic tools now provide access to analogues with improved activity and ease of access,[4] a detailed understanding of the mechanisms by which the ritterazines and cephalostatins induce tumor cell apoptosis remains unclear.[5] Recent studies from a team led by Shair suggest that **1** and **2** target an oxysterol binding protein (OSBP);

[†] Purdue University.
[‡] Xenobe Research Institute.

(1) (a) Pettit, G. R.; Inoue, M.; Kamano, Y.; Herald, D. L.; Arm, C.; Dufresne, C.; Christie, N. D.; Schmidt, J. M.; Doubek, D. L.; Krupa, T. S. *J. Am. Chem. Soc.* **1988**, *110*, 2006–2007. (b) Fukuzawa, S.; Matsunaga, S.; Fusetani, N. *J. Org. Chem.* **1994**, *59*, 6164–6166.

(2) (a) Moser, B. R. *J. Nat. Prod.* **2008**, *71*, 487–491. (b) Flessner, T.; Jautelat, R.; Scholz, U.; Winterfeldt, E. *Fortschr. Chem. Org. Naturst.* **2004**, *87*, 1–80. (c) Lee, S.; LaCour, T. G.; Fuchs, P. L. *Chem. Rev.* **2009**, *109*, 2275–2314.

(3) (a) Jeong, J. U.; Sutton, S. C.; Kim, S.; Fuchs, P. L. *J. Am. Chem. Soc.* **1995**, *117*, 10157–10158. (b) Fortner, K. C.; Kato, D.; Tanaka, Y.; Shair, M. D. *J. Am. Chem. Soc.* **2010**, *132*, 275–280.

(4) (a) Lee, S.; LaCour, T. G.; Fuchs, P. L. *Chem. Rev.* **2009**, *109*, 2275–314. (b) Phillips, S. T.; Shair, M. D. *J. Am. Chem. Soc.* **2007**, *129*, 6589–6598.

10.1021/ol202139z
Published on Web 09/14/2011

however, a link between this target and the apoptotic activity of **1** and **2** has yet to be established.[6]

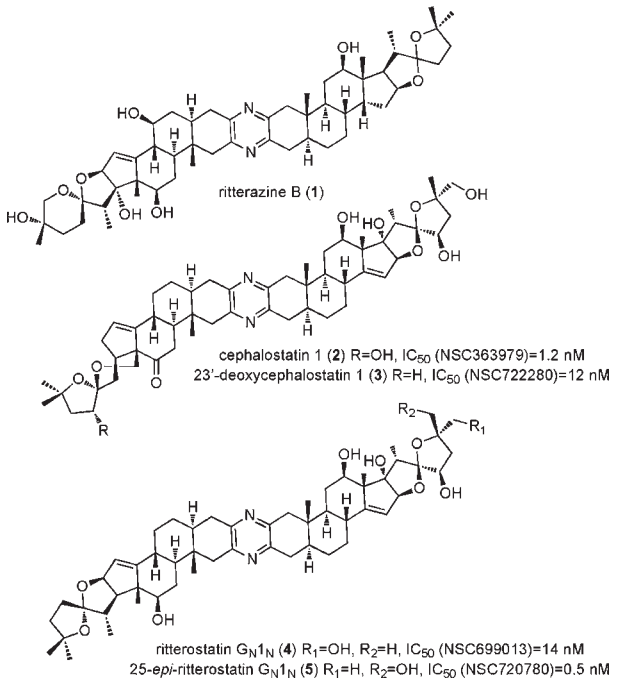

Figure 1. Structures of ritterazine B (**1**), cephalostatin 1 (**2**), 23′-deoxycephalostatin 1 (**3**), ritterostatin G_N1_N (**4**), and 25-*epi*-ritterostatin hybrid G_N1_N (**5**).

Our ability to synthesize cephalostatin, ritterazine, and hybrid analogues has been used to supply sufficient quantities of materials for detailed biological and in vivo studies. For instance, the first-generation synthesis of 110 mg of 23′-deoxycephalostatin 1 (**3**) was used to characterize their apoptotic activity and evaluate the accompanying mitochondrial damage and cytosolic Ca^{2+} increase.[7] These studies have also shown that **3** engenders a 50−60% increase in mouse lifespan in U87MG brain cancer xenografts.[8] Synthetic samples (from 245 mg total) of 25-*epi*-ritterostatin G_N1_N (**5**) were further screened for in vitro activity against multiple cancer cells lines of different tissue origins.[3a,4a]

Given our synthetic access, application of these materials to prepare and evaluate fluorescent probes was a logical next step. Our unsymmetrical pyrazine synthetic route operates through a coupling of a α-azidoketone and a α-aminomethoxime.[4a] Since both steroidal precursors pass through the α-azidoketone stage, there are two coupling modes to the same product. The bottom line is that this unsymmetrical pyrazine synthesis provides dependable late-stage coupling of an exceptionally valuable pair of 3-ketosteroids with the expectation of excellent overall yield and preservation of acid-labile spiroketal stereochemistry. The average yield for the initial 59 cases examined was 72%.

Using SAR studies as a guide,[9] the C-25 position was targeted, as it has shown tolerance to modification. Our studies focused on use of an immunoaffinity fluorescent (IAF) label,[10] as this label has been shown to provide effective probes without phenotypic modification and modest loss in cell viability and activity.

Scheme 1. Synthesis of IAF-Labeled Fluorescent Probe **7**

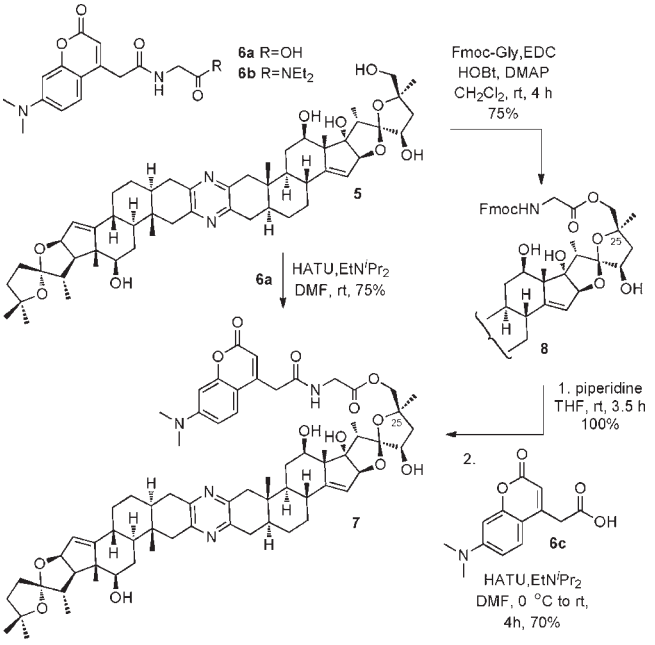

Glycine IAF label **6a**[11] was coupled with 25-*epi*-ritterostatin G_N1_N (**5**) at the C-25 position to deliver probe **7** (Scheme 1). The same probe **7** was also obtained through a stepwise procedure involving an Fmoc-protected intermediate **8**.

Using the MTT assay, probe **7** demonstrated an activity of IC_{50} value of 79 ± 4 nM against HCT-116 cells.[12] With

(5) (a) Rudy, A.; López-Antón, N.; Dirsch, V. M.; Vollmar, A. M. J. *Nat. Prod.* **2008**, *71*, 482–486. (b) Komiya, T.; Fusetani., T.; Matsunaga, S.; Kubo, A.; Kaye, F. J.; Kelley, J. M.; Tamura, K.; Yoshida, M.; Fukuoka, M.; Nakagawa, K. *Cancer Chemother. Pharmacol.* **2003**, *51*, 202–208.

(6) Burgett, A. W.; Poulsen, T. B.; Wangkanont, K.; Anderson, D. R.; Kikuchi, C.; Shimada, K.; Okubo, S.; Fortner, K. C.; Mimaki, Y.; Kuroda, M.; Murphy, J. P.; Schwalb, D. J.; Petrella, E. C.; Cornella-Taracido, I.; Schirle, M.; Tallarico, J. A.; Shair, M. D. *Nat. Chem. Biol.* **2011**, *7*, 639–647.

(7) Unpublished results with Prof. Peng Huang (M. D. Anderson).

(8) (a) Unpublished studies with Dr. John Beutler (National Cancer Institute). (b) Synthesis of 25-*epi*-ritterostatin G_N1_N will be reported in due course.

(9) (a) LaCour, T. G.; Guo, C.; Ma, S.; Jeong, J. U.; Boyd, M. R.; Matsunaga, S.; Fusetani, N.; Fuchs, P. L. *Bioorg. Med. Chem. Lett.* **1999**, *9*, 2587–2592. (b) Guo, C.; LaCour, T. G.; Fuchs, P. L. *Bioorg. Med. Chem. Lett.* **1999**, *9*, 419–424.

(10) Yu, W. L.; Guizzunti, G.; Foley, T. L.; Burkart, M. D.; La Clair, J. J. *J. Nat. Prod.* **2010**, *73*, 1659–1666.

(11) (a) Hughes, C. C.; MacMillan, J. B.; Gaudêncio, S. P.; Fenical, W.; La Clair, J. J. *Angew. Chem., Int. Ed.* **2009**, *48*, 728–732. (b) Alexander, M. D.; Burkart, M. D.; Leonard, M. S.; Portonovo, P.; Liang, B.; Ding, X.; Joullié, M. M.; Gulledge, B. M.; Aggen, J. B.; Chamberlin, A. R.; Sandler, J.; Fenical, W.; Cui, J.; Gharpure, S. J.; Polosukhin, A.; Zhang, H. R.; Evans, P. A.; Richardson, A. D.; Harper, M. K.; Ireland, C. M.; Vong, B. G.; Brady, T. P.; Theodorakis, E. A.; La Clair, J. J. *ChemBioChem* **2006**, *7*, 409–416.

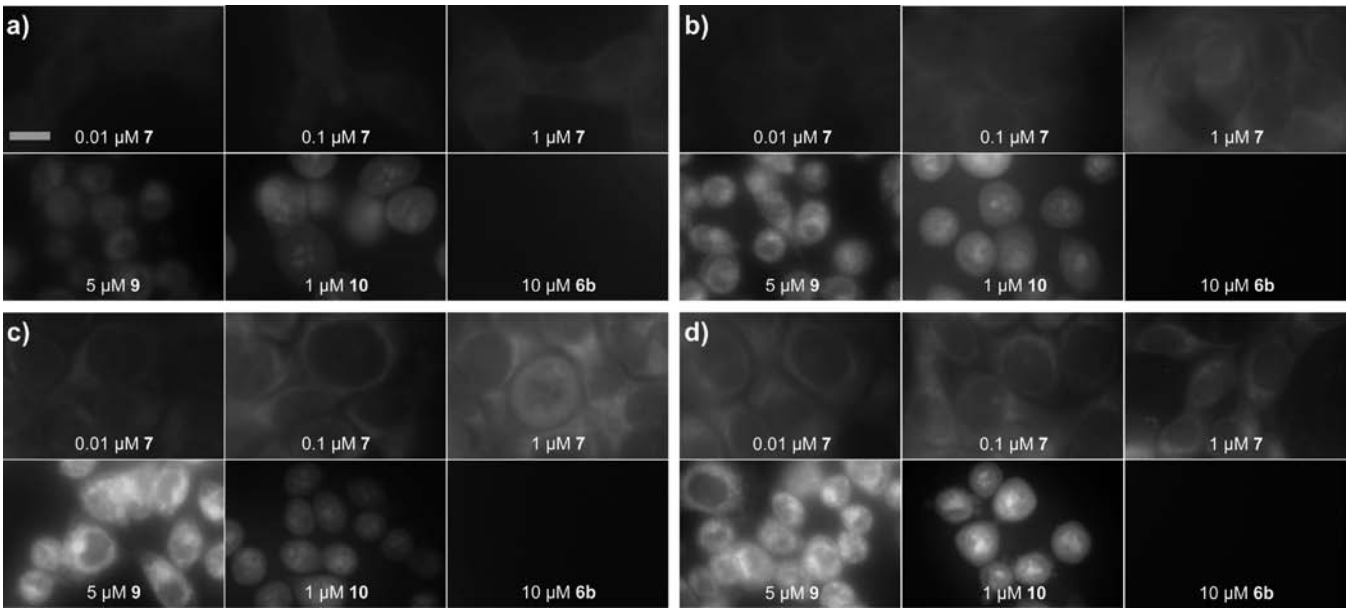

Figure 2. Time-course imaging depicting the uptake and subcelluar localization of probe **7** in live HCT-116 cells. Images were collected using a custom built fiberoptic microscope (see the Supporting Information) that was mounted on a computer-driven XYZ micrometer adjustable stage and was equipped to excite with an LED at λ_{ex} = 380 nm and collect emission at λ_{em} = 448 ± 20 nm. Images were collected at 30 min intervals over a 24 h period using identical optical parameters. A concentration gradient of each probe was conducted and compared to cells treated with dragmacidin D (**9**), an ER stain, and IAF-labeled nogalamycin (**10**), a nuclear stain and an IAF control, compound **6b**. Images are provided at (a) 1 h, (b) 6 h, (c) 12 h, and (d) 24 h. Bar denotes 10 μm.

active probe and access to panel of IAF-labeled natural products and controls,[11b] our studies shifted to develop a detailed description of the uptake and subcellular localization of **7**.

Using inexpensive components, a live cell imaging system was built containing a polycarbonate CO_2 incubator mounted on the head of computer-driven fiberoptic microscope (see the Supporting Information). The instrument was designed to rapidly capture images from 24 experiments in parallel at 30 min intervals over a 24 h period. In this system, the uptake of three concentrations of probe **7** was measured in triplicate along the respective positive and negative controls (Figure 2).

An identical outcome was observed after multiple of repetitions. After 6 h, probe **7** appeared in the nuclear membrane and extending into the endoplasmic reticulum (ER). The intensity of this stain increased until 12 h where it remained consistent thereafter (imaging was conducted up to 24 h). This localization was confirmed by comparison with a complementary blue-fluorescent nuclear stain, IAF-labeled nogalamycin (**10**),[8b] and blue-fluorescent ER stain dragmacidin D (**9**) (structures of **9** and **10** are provided in the Supporting Information).[13] Further controls indicated that the label alone did not stain cells under identical conditions.[14] Even at concentrations up to 250 μM, the lack of fluorescence from controls such as **6b** (Scheme 1) in live cells indicated that the uptake and localization was indeed due to the natural product's activity.

While time course imaging served for initial analyses, confocal microscopy provided improved resolution. Using the data from the time course studies, HCT-116 cells were treated with 0.1 μM **7** for 12 h, washed with media, and imaged. These studies provided further support for the localization in the endoplasmic reticulum (er, Figure 3a) and around the nuclear membrane (nm, Figure 3a). However, probe **7** was also observed on chromatin (label c, Figure 3a) within the nucleus of HCT-116 cells. By evaluating other cell lines, this observation was linked to a unique selectivity in HCT-116 cells. For example, probe **7** was not localized on chromatin in HeLa cells (label c, Figure 3b).

While control experiments indicated the label did not alter the subcellular localization, further studies were conducted to confirm the localization of probe **7** was comparable to ritterazine B (**1**) or celphalostatin 1 (**2**). Both **1** and **2** were shown to effectively block the uptake of probe **7** (as shown in Figure 3c,d).

This observation suggests two key points. First, ritterazine B (**1**) as well as probe **7** bind to their target in a strong and irreversible manner (if this was not the case treatment of cells exposed to **1** with probe **7**, as in Figure 3c or d, would have led to comparable localization as in Figure 3a).

(12) Activities were measured using the protocols described in: Kang, M.; Jones, B. D.; Mandel, A. L.; Hammons, J. C.; DiPasquale, A. G.; Rheingold, A. L.; La Clair, J. J.; Burkart, M. D. *J. Org. Chem.* **2009**, *74*, 9054–9061.

(13) Forsyth, C. J.; Ying, L.; Chen, J.; La Clair, J. J. *J. Am. Chem. Soc.* **2006**, *128*, 3858–3859.

(14) See examples: La Clair, J. J. *Nat. Prod. Rep.* **2010**, *27*, 969–995.

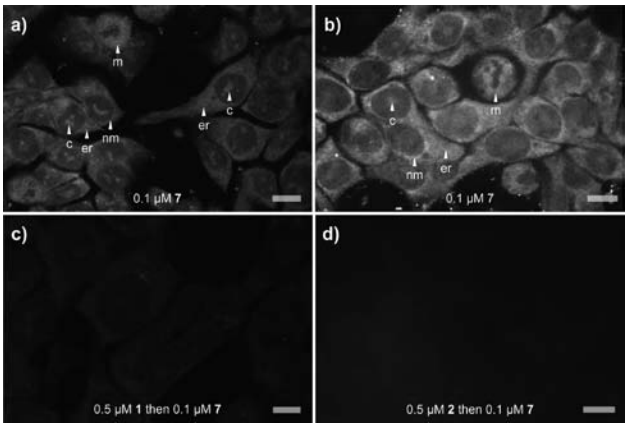

Figure 3. Confocal fluorescent images detailing the subcellular localization of probe **7** and corresponding natural products ritterazine B (**1**) or celphalostatin 1 (**2**): (a) live HCT-116 cells that were incubated with probe **7** for 12 h; (b) comparable uptake arising from treating HeLa cells with probes **7** for 12 h; (c) HCT-116 cells that were treated with ritterazine B (**1**) for 12 h followed by probe **7** for an additional 12 h; (d) HCT-116 cells that were treated with cephalostatin 1 (**2**) for 12 h followed by probe **7** for an additional 12 h. Labels denote chromatin (c), endoplasmic reticulum (er), nuclear membrane (nm), and mitotic cell (m). Images were collected with excitation at λ_{ex} = 405 nm and emission at λ_{em} = 448 ± 20 nm. Bars denote 10 μm.

Second, and perhaps most importantly, probe **7** shares a common target with ritterazine **1** and cephalostatin **2**. While suggested by related hybrid natural products,[15] this study provides direct evidence that the cephalostatins, ritterazines, and hybrids of both natural products share a common mode of action.

(15) (a) Suzuki, K. *Chem. Rec.* **2010**, *10*, 291–307. (b) Meunier, B. *Acc. Chem. Res.* **2008**, *41*, 69–77.

(16) Ellenberg, J.; Siggia, E. D.; Moreira, J. E.; Smith, C. L.; Presley, J. F.; Worman, H. J.; Lippincott-Schwartz, J. *J. Cell. Biol.* **1997**, *138*, 1193–1206.

Further insight into the cellular targeting was obtained from examining mitotic cells treated with **7** (m, Figure 3b). While localizing on chromatin in mature cells, probe **7** was not observed binding to the chromosomes during mitosis. As illustrated in Figure 3b, fluorescence from **7** was observed in the cytosolic space prophase to telophase. This observation was consistent with the transitioning of the nuclear envelope and ER membranes during mitosis.[16]

In summary, this study describes the preparation of a fluorescent probe based on a ritterazine–cephalostatin hybrid. Time course and confocal microscopy indicate that a ritterazine–cephalostatin hybrid probe shares a common uptake and subcellular localization in the ER, nuclear membrane, and chromatin with ritterazine B (**1**) and cephalostain 1 (**2**). The observed uptake and subcellular localization was consistent with the transitioning during mitosis.[13]

The study further illustrates how scarce natural materials made available through complex chemical synthesis play a pivotal role in evaluating natural product activity. Our program is now focused on applying these materials to identify the molecular targets and pathways modulated by this unique class of bis-steroidal alkaloid, with the goal of identify the pathways regulated by probe **7** during cell growth and division.

Acknowledgment. This work was supported by funding from the NIH (5U01CA060548-17 and CA 60548) and internal support from XRI. We sincerely thank Dr. Douglas Lantrip for laboratory assistance and Dr. Karl Wood and Arlene Rothwell of Purdue University for assistance with collection of the mass spectral data.

Supporting Information Available. Synthetic procedures, copies of NMR spectra on the probes, as well as detailed procedures for the cellular imaging studies and time course imaging system are available. This material is available free of charge via the Internet at http://pubs.acs.org.